

Mean-field dynamics of a quantum dot - microcavity system

Herbert Vinck-Posada⁽¹⁾, Boris A. Rodriguez⁽¹⁾, Augusto Gonzalez^(1,2)

⁽¹⁾*Instituto de Física, Universidad de Antioquia, AA 1226, Medellín, Colombia*

⁽²⁾*Instituto de Cibernética, Matemática y Física, Calle E 309, Vedado, Ciudad Habana, Cuba*

Mean-field evolution equations for the exciton and photon populations and polarizations (Bloch-Lamb equations) are written and numerically solved in order to describe the dynamics of electronic states in a quantum dot coupled to the photon field of a microcavity. The equations account for phase space filling effects and Coulomb interactions among carriers, and include also (in a phenomenological way) incoherent pumping of the quantum dot, photon losses through the microcavity mirrors, and electron-hole population decay due to spontaneous emission of the dot. When the dot may support more than one electron-hole pair, asymptotic oscillatory states, with periods between 0.5 and 1.5 ps, are found almost for any values of the system parameters.

PACS numbers: 78.67.Hc, 42.50.Ct

Keywords: dynamics, quantum dot, microcavity

I. INTRODUCTION

The coupling of light with an atomic state depends basically on two factors: (a) the spread of the wave function or dipole moment of the atomic state, and (b) the density of photon states in the energy region of interest. In the search for optimizing this coupling, atomic Rydberg states and three-dimensional microcavities, where the photon modes exhibit a discrete spectrum, have been used. One of the salient realizations is the construction of micromasers¹.

More recently, excitonic states in quantum dots have proven to be excellent candidates to replace atomic Rydberg states in a microcavity. From one side, quantum dots can easily be incorporated inside the microcavity by means of modern semiconductor technology, thus avoiding the complicated step in which a beam of atoms in Rydberg states is prepared. On the other hand, the effective Bohr radius in a semiconductor is a factor of $m_0\epsilon/(m\epsilon_0)$ larger than the corresponding radius in vacuum, where m_0 and ϵ_0 are, respectively, the electron mass and dielectric constant of vacuum, and m , ϵ are the corresponding magnitudes in the semiconductor. In GaAs, for example, this factor is around 200. As a result, the ground-state exciton wave function is as spread as an atomic Rydberg state. Transitions energies are typically in the infrared range.

In the present paper, we study the dynamics of a quantum dot-microcavity system, focusing on the stationary or asymptotic photonic states in the cavity. A previous, very serious, study of this dynamics² has been motivated by recent experimental work^{3,4,5}, and theoretical papers^{6,7}, in which the exciton-cavity coupling is characterized, and the system is shown to serve as an efficient source of single triggered photons, and a possible source of entangled photons.

The results of Ref. 2 rely on the assumption that the quantum dot may support only one excitonic state (a shallow dot). We relax this assumption, allowing more than one excitonic state in the dot. Coulomb interactions among particles are shown to play an important

role in the dynamics, shifting the single-pair levels, modifying the Rabi frequencies, and causing interference effects. The most relevant consequence of including additional pair states in the dot, however, is shown to be the existence of asymptotic oscillatory states, in which the number of photons oscillates around a mean value, with periods between 0.5 and 1.5 ps (for the set of parameters used in the calculations). We keep the assumption that the excitonic states are coupled to a single photon mode. This means that the separation between photon modes in the cavity should be larger than the splitting between excitonic states in the dot. As the latter magnitude is of the order of a few meV, our results will be valid for cavities with a radius of 0.5 μm or smaller⁸.

A second, simplifying, working hypothesis is the mean field approximation. For electrons, it means the neglect of correlation terms in the evolution (Bloch) equations. For light, we use a semiclassical or coherent (Lamb) description, in which the field is characterized by an amplitude and a phase. Let us stress that, in the intervals of parameters we consider, when the number of photons proves to be significantly different from zero the statistics of the photon field is Poissonian or near Poissonian, at least in the one-exciton dot², in such a way that the coherent approximation for the photon field is justified. The reward from this simplification is that the system of evolution equations is relatively small, allowing a qualitative analysis of its solutions, and the extension to deeper dots, which may support more than one electron-hole states.

The plan of the paper is as follows. In Sec. II, the basic evolution (Bloch-Lamb) equations are obtained, and the initial conditions used to solve them are discussed. Sec. III is devoted to the presentation of results. The one-, two-, and three-states dots coupled to a single photon mode (with a given polarization) are studied. Additionally, the two-states dot coupled to a polarization degenerated light mode is also considered. Finally, concluding remarks are given in Sec. IV.

II. THE THEORY

Our model microcavity is assumed to have an ideal cylindrical shape. Its radius is lower than $0.5 \mu\text{m}$, in such a way that the spacing between photon modes is of the order of 20 meV .⁸ We will be interested in one of these modes. To fix ideas, we speak about the lowest mode, polarization degenerated, which is called HE_{11} according to the terminology for modes in a guide⁹. In the paper, we will conventionally denote the two polarization components as $\sigma_{(+)}$ and $\sigma_{(-)}$.

A quantum dot is located at a point along the cavity axis in which the electric field has a maximum. We assume a GaAs dot. The dot has also a cylindrical shape. Its height is lower than 10 nm , in such a way that light-hole sub-bands have higher energy than the heavy-hole ones and, in a first approximation, could be ignored in the dynamics. A second reason for not including light holes is that their coupling to the photon modes is a factor of 3 less intense than the heavy hole coupling¹⁰.

Electron-hole pairing is induced by both Coulomb interactions and the coupling to the photon mode. Thus, in addition to the electron, hole and photon populations:

$$\rho_{nn}^{(e)} = \langle e_n^\dagger e_n \rangle, \quad (1)$$

$$\rho_{\bar{n}\bar{n}}^{(h)} = \langle h_{\bar{n}}^\dagger h_{\bar{n}} \rangle, \quad (2)$$

$$|\sigma_{(+)}|^2 = \langle a_{(+)}^\dagger a_{(+)} \rangle, \quad (3)$$

$$|\sigma_{(-)}|^2 = \langle a_{(-)}^\dagger a_{(-)} \rangle, \quad (4)$$

there are nontrivial pairing or polarization functions:

$$\kappa_{n\bar{n}}^{(+)} = \langle e_{n\downarrow} h_{\bar{n}\uparrow} \rangle, \quad (5)$$

$$\kappa_{n\bar{n}}^{(-)} = \langle e_{n\uparrow} h_{\bar{n}\downarrow} \rangle. \quad (6)$$

In these equations, n and \bar{n} label electron and hole single-particle states in the dot. e_n^\dagger and $h_{\bar{n}}^\dagger$ are the corresponding creation operators. $a_{(+)}$ and $a_{(-)}$ are operators for the two photon polarizations. In the κ functions, we have explicitly indicated the electron and hole states that are coupled to a polarized mode. For example, in $\kappa^{(+)}$ the coupling of a spin-down electron state ($m_j = -1/2$) with a ‘‘spin-up’’ hole state (coming from a $m_j = -3/2$ electron state in the valence band) is due to the $\sigma_{(+)}$ mode, and it is reinforced by Coulomb interactions.

Notice also that we have assumed pairing between specific electron and hole states, n and \bar{n} (orbitals). We will use a harmonic oscillator basis. Thus, for a given n characterized by radial and angular momentum projection quantum numbers, $n = (k, l)$, the hole state coupled to n is $\bar{n} = (k, -l)$. The pair is created in a zero total angular momentum state, corresponding to the selection rule for interband transitions¹⁰.

Mean values, $\langle \dots \rangle$, come from averaging with a density matrix. We are interested in the very low temperature, $T \rightarrow 0$ limit. This density matrix is time dependent. Thus, the population and polarization functions, Eqs. (1-6), are time-dependent functions. We will derive dynamical equations for their time evolution (Bloch-Lamb equations).

A further simplification equates $\rho_{nn}^{(e)} = \rho_{\bar{n}\bar{n}}^{(h)} = \rho_n$. This means that the dot is initially neutral, and that we are interested in the dynamics over a time interval smaller than (or of the order of) the relaxation times in the dot (the coherent regime¹¹). In fact, we will follow the dynamics in the time interval $(0, 20 \text{ ps})$.

The Hamiltonian describing the quantum dot - microcavity system can be written in the following form:

$$\begin{aligned} H = & \sum_n \left(E_n^{(e)} e_n^\dagger e_n + E_{\bar{n}}^{(h)} h_{\bar{n}}^\dagger h_{\bar{n}} \right) + \sum_{k,n} \left(t_{kn}^{(e)} e_k^\dagger e_n + t_{k\bar{n}}^{(h)} h_k^\dagger h_{\bar{n}} \right) + \frac{\beta}{2} \sum_{rsuv} \langle r, s | \frac{1}{r} | u, v \rangle e_r^\dagger e_s^\dagger e_v e_u \\ & + \frac{\beta}{2} \sum_{rsuv} \langle r, s | \frac{1}{r} | u, v \rangle h_r^\dagger h_s^\dagger h_{\bar{v}} h_{\bar{u}} - \beta \sum_{rsuv} \langle r, \bar{s} | \frac{1}{r} | u, \bar{v} \rangle e_r^\dagger h_s^\dagger h_{\bar{v}} e_u + \hbar\omega \left(a_{(+)}^\dagger a_{(+)} + a_{(-)}^\dagger a_{(-)} \right) \\ & + g \sum_n \left\{ a_{(+)}^\dagger e_{n\downarrow} h_{\bar{n}\uparrow} + a_{(+)} h_{\bar{n}\uparrow}^\dagger e_{n\downarrow} \right\} + g \sum_n \left\{ a_{(-)}^\dagger e_{n\uparrow} h_{\bar{n}\downarrow} + a_{(-)} h_{\bar{n}\downarrow}^\dagger e_{n\uparrow} \right\}. \end{aligned} \quad (7)$$

The E_n functions refer to the single-particle energies of the used basis states. On the other hand, t_{kn} are the matrix elements of the external (quantum dot) confinement potential. β is the strength of Coulomb interactions, and g the strength of the electron-photon coupling (assumed constant). The energy of the photon mode is written as $\hbar\omega$.

A. Bloch-Lamb equations

The dynamical equations are obtained by taking time derivatives of the occupation and polarization functions (1-6). One gets for ρ_n , for example:

$$i\hbar \frac{d\rho_n}{dt} = \langle [e_n^\dagger e_n, H] \rangle. \quad (8)$$

Once the commutator is computed, we take the mean-field or quasiparticle contribution (in which mean values of products of four or more operators are expressed in terms of products of occupations and polarization functions), and neglect the collision terms¹¹. The result for $\rho_{n\downarrow}$ is:

$$\begin{aligned} \frac{d\rho_{n\downarrow}}{dt} = & -\frac{2\beta}{\hbar} \text{Im} \left(\kappa_{n\bar{n}}^{(+)*} \sum_j \langle n, j | 1/r | j, n \rangle \kappa_{j\bar{j}}^{(+)} \right) \\ & - \frac{2g}{\hbar} \text{Im} \left(\sigma_{(+)}^* \kappa_{n\bar{n}}^{(+)} \right), \end{aligned} \quad (9)$$

and a similar equation for $\rho_{n\uparrow}$. Notice that Coulomb interactions preserve spin. Thus, if n is a spin-down state (as assumed in Eq. (9)), the j states entering the sum should be spin-down states also. This is the reason why only $\kappa^{(+)}$ functions enter the sum.

The equation for the photon number is straightforwardly obtained also, and leads to:

$$\frac{d|\sigma_{(+)}|^2}{dt} = \frac{2g}{\hbar} \text{Im} \left(\sum_j \sigma_{(+)}^* \kappa_{j\bar{j}}^{(+)} \right). \quad (10)$$

Notice the conservation of the polariton number, as it follows from Eqs. (9) and (10) (or directly from the Hamiltonian, Eq. (7)): $dN_{pol}^{(+)} / dt = 0$, where:

$$N_{pol}^{(+)} = |\sigma_{(+)}|^2 + \sum_n \rho_{n\downarrow}. \quad (11)$$

The equations for the polarization functions, κ , are obtained in the same way. We shall stress, however, that the modulus, $|\kappa|$, is determined from Eq. (9), and it follows that $|\kappa_{n\bar{n}}^{(+)}| = \sqrt{\rho_{n\downarrow}(1 - \rho_{n\downarrow})}$. Nevertheless, we are forced to use the equation for $\kappa_{n\bar{n}}^{(+)}$ in order to determine its phase.

In the same way, the modulus of $\sigma_{(+)}$ (understood as $\langle a_{(+)} \rangle$) is determined by Eq. (10), but its phase is not. Thus, we must write the equation for $\sigma_{(+)}$.

Both σ and κ should contain a rapidly varying phase factor, $e^{-i\omega t}$, due simply to the frequency of rotation of the electric field. For example, $\omega \sim 2 \times 10^3 \text{ ps}^{-1}$ for the GaAs band gap. In contrast, we expect characteristic frequencies of the order of $g/\hbar \sim 1 \text{ ps}^{-1}$ in the variation of ρ_n or $|\sigma|$. Thus, we will use a kind of Rotating Wave Approximation, and write explicitly the trivial (rapid) phase dependence of σ and κ :

$$\sigma_{(+)} = s_{(+)} e^{-i\omega t - i\phi^{(+)}} , \quad (12)$$

$$\kappa_{n\bar{n}}^{(+)} = \kappa_n^{(+)} e^{-i\omega t - i\phi_n^{(+)}} , \quad (13)$$

etc. By definition, $s_{(+)} = |\sigma_{(+)}|$, and $\kappa_n^{(+)} = |\kappa_{n\bar{n}}^{(+)}|$. The equations for ϕ and ϕ_n are, then:

$$\frac{d\phi^{(+)}}{dt} = \frac{g}{\hbar s_{(+)}} \sum_j \kappa_j^{(+)} \cos(\phi^{(+)} - \phi_j^{(+)}) , \quad (14)$$

$$\begin{aligned} \frac{d\phi_n^{(+)}}{dt} = & - \left\{ \omega - \frac{1}{\hbar} \left(E_{gap} + E_n^{(e)} + E_{\bar{n}}^{(h)} + t_{nn}^{(e)} + t_{\bar{n}\bar{n}}^{(h)} \right) + \frac{\beta}{\hbar} \langle n, n | 1/r | n, n \rangle + \frac{2\beta}{\hbar} \sum_{j \neq n} \langle n, j | 1/r | j, n \rangle \rho_{j\downarrow} \right\} \\ & + \frac{\beta}{\hbar \kappa_n^{(+)}} (2\rho_{n\downarrow} - 1) \sum_{j \neq n} \langle n, j | 1/r | j, n \rangle \kappa_j^{(+)} \cos(\phi_n^{(+)} - \phi_j^{(+)}) - \frac{g s_{(+)}}{\hbar \kappa_n^{(+)}} (2\rho_{n\downarrow} - 1) \cos(\phi_n^{(+)} - \phi^{(+)}) , \end{aligned} \quad (15)$$

and similar equations for $\phi^{(-)}$ and $\phi_n^{(-)}$. We may easily identify in Eqs. (14,15) the space-filling factors, $2\rho_n - 1$, mean-field contributions to the pair energies, detuning factors, etc.

Eqs. (9,15) are Bloch equations for the electronic occupations and polarizations in the quantum dot¹¹, in a mean field approximation and under a coherent regime, whereas (10,14) are the analogues of the semiclassical Lamb equations for a laser¹². Thus, we will call our system of evolution equations Bloch-Lamb equations. Losses and incoherent pumping are introduced in the next subsection.

B. Phenomenological account of pumping and losses

The main processes of the interaction between the quantum dot - microcavity system and the external medium are described in Ref. 2, and modeled by means of additional terms in the Liouville equation for the density matrix.

One of such processes is the decay of cavity photons by escaping through the cavity mirrors. We may account for this process by introducing a decay term, $-\varkappa |\sigma_{(+)}|^2$, into Eq. (10), with a phenomenological decay rate, \varkappa . Roughly, we have $\varkappa \sim \hbar\omega/Q$, where the quality factor of the cavity is in the range between 1000 and 5000.³

In terms of the variables introduced in Eqs. (12,13), the modified Eq. (10) is, thus, rewritten:

$$\frac{ds_{(+)}}{dt} = \frac{g}{\hbar} \sum_j \kappa_j^{(+)} \sin(\phi^{(+)} - \phi_j^{(+)}) - \varkappa s_{(+)}/2. \quad (16)$$

On the other hand, the electronic population, $\rho_{n\downarrow}$,

$$\begin{aligned} \frac{d\rho_{n\downarrow}}{dt} = & - \frac{2\beta}{\hbar} \kappa_n^{(+)} \sum_{j \neq n} \langle n, j | 1/r | j, n \rangle \kappa_j^{(+)} \sin(\phi_n^{(+)} - \phi_j^{(+)}) - \frac{2g}{\hbar} s_{(+)} \kappa_n^{(+)} \sin(\phi^{(+)} - \phi_n^{(+)}) \\ & - \gamma \rho_{n\downarrow} + P_{(+)}(1 - \rho_{n\downarrow}). \end{aligned} \quad (17)$$

The set of equations (14-17) determine the magnitudes $\rho_{n\downarrow}$, $s_{(+)}$, $\phi^{(+)}$, and $\phi_n^{(+)}$. $\kappa_n^{(+)}$ is obtained in terms of $\rho_{n\downarrow}$ as $\sqrt{\rho_{n\downarrow}(1 - \rho_{n\downarrow})}$. Notice that the phase of $\kappa_n^{(+)}$ is not affected by the decay processes in this approximation. The modulus of $\kappa_n^{(+)}$ decays at a rate which is determined by the decay of $\rho_{n\downarrow}$. This is the analogue of the relation $T_2 = 2T_1$ between the decay times of populations and coherences, valid both in Atomic Physics¹² and, in a certain way, in bulk semiconductors¹¹. Let us stress also that the r.h.s. of Eqs. (14-17) depend only on differences of angles. Thus, we may eliminate one of the angles, for example ϕ , by introducing the new variables $\theta_n = \phi - \phi_n$.

A formally similar set of equations may be written for $\rho_{n\uparrow}$, $s_{(-)}$, $\phi^{(-)}$, and $\phi_n^{(-)}$. Notice that, in our approximation, where Coulomb collision terms and other relaxation processes (due to the interaction with phonons, impurities, etc) are neglected, the relations $\rho_{nn}^{(e)} = \rho_{\bar{n}\bar{n}}^{(h)}$ are preserved at all times, and $\rho_{n\downarrow}$ evolves independently of $\rho_{n\uparrow}$.

C. The $t \rightarrow 0$ asymptotics

Eqs. (14-17) are to be solved with null initial conditions, i.e., there are no pairs in the quantum dot and no photons in the cavity at $t = 0$.

According to Eq. (17), the populations $\rho_{n\downarrow}$ rise as $P_{(+)}t$ and, consequently, $\kappa_n^{(+)} \sim \sqrt{P_{(+)}t}$. However, the small- t asymptotics of the magnitudes $s_{(+)}$, $\phi^{(+)}$ and $\phi_n^{(+)}$ should be analysed with care because of terms like $\kappa_n^{(+)} / s_{(+)}$, etc entering the equations. We found that the consistent behavior in the $t \rightarrow 0$ limit is the following:

$$\rho_{n\downarrow} = P_{(+)}t + \dots, \quad (18)$$

$$\kappa_n^{(+)} = \sqrt{P_{(+)}t} + \dots, \quad (19)$$

is modified by a continuous incoherent pumping of the quantum dot at a rate $P_{(+)}$, and the decay of electron-hole pairs by spontaneous emission into leaky modes at a rate γ . In Eq. (9), one should add the following terms: $P_{(+)}(1 - \rho_{n\downarrow}) - \gamma \rho_{n\downarrow}$, where Pauli blocking is explicitly introduced in the pumping contribution. The resulting equation for $\rho_{n\downarrow}$ is, then:

$$s_{(+)} = \frac{2gN_{states}}{3\hbar} \sqrt{P_{(+)}} t^{3/2} + \dots, \quad (20)$$

$$\phi_n^{(+)} = a_n^{(+)}t + \dots, \quad (21)$$

$$\phi^{(+)} = \pi/2 + a_\phi^{(+)}t + \dots, \quad (22)$$

where N_{states} is the number of single-particle states available in the dot, and

$$\begin{aligned} a_n^{(+)} = & -\omega + \frac{1}{\hbar} (E_{gap} + E_n^{(e)} + E_n^{(h)} + t_{nn}^{(e)} + t_{\bar{n}\bar{n}}^{(h)}) \\ & - \frac{\beta}{\hbar} \sum_j \langle n, j | 1/r | j, n \rangle, \end{aligned} \quad (23)$$

$$a_\phi^{(+)} = \frac{3}{5N_{states}} \sum_n a_n^{(+)}. \quad (24)$$

n and j in Eqs. (23-24) represent spin-down states. Eqs. (18-24) are to be used in the numerical integration of Eqs. (14-17).

III. NUMERICAL RESULTS

In order to perform the numerical integration of Eqs. (14-17), we shall give a precise meaning to the magnitudes entering them. We are interested in a quantum dot which supports a finite number of single-particle states, N_{states} . Thus, N_{states} will be fixed by hand. A magnetic field, $B = 7$ Teslas, acts on the charge carriers in the dot. Both, the dot confinement and the magnetic field may be thought of as control parameters. Energy magnitudes are converted to angular frequencies by dividing by \hbar .

We will use parameters for GaAs. The single-particle energies are defined as:

$$\begin{aligned} E_n^{(e,h)} = & \frac{\hbar\omega_c^{(e,h)}}{2} (2k_n \pm l_n + |l_n| + 1) \\ & \pm g_{e,h} \mu_B B S_{zn}^{(e,h)}, \end{aligned} \quad (25)$$

where the cyclotron frequencies are $\omega_c^{(e)} = 2.625 B \text{ ps}^{-1}$, $\omega_c^{(h)} = 1.173 B \text{ ps}^{-1}$ (and B in Teslas). $S_z = \pm 1/2$ are the spin projections along B . $g_e \mu_B / (2\hbar) = 4.397 \times 10^{-3} \text{ ps}^{-1}$, and $g_h \mu_B / (2\hbar) = -4.397 \times 10^{-2} \text{ ps}^{-1}$. The + sign in Eq. (25) corresponds to the electron. The fact that, in our simple model, energy levels come from a parabolic confinement and a magnetic field has not a decisive importance. What really matters is the position of the bare levels, and the effects of Coulomb interaction among carriers, as will become evident in the next sections.

On the other hand, the matrix elements of the (parabolic) confinement potential are written as:

$$t_{nn}^{(e,h)} = \frac{\hbar \omega_0^2}{\omega_c^{(e,h)}} (2k_n + |l_n| + 1), \quad (26)$$

where the dot frequency is $\omega_0 = 4.558 \text{ ps}^{-1}$. The electron-photon coupling, g , which determines the Rabi frequency, is fixed to $g/\hbar = 1.5 \text{ ps}^{-1}$, and the strength of Coulomb interactions is $\beta/\hbar = 3.871\sqrt{B} \text{ ps}^{-1}$.

Notice that we have not included the nominal gap energy into the electron energy, Eq. (25). A shifted mode frequency is defined according to $\Delta = \omega - E_{gap}/\hbar$.

Concerning the loss and pumping parameters introduced in Sec. II B, we will set the rate of spontaneous decay, γ , to 0.1 ps^{-1} . The equations are integrated for different sets of P , \varkappa , and Δ . A variation of Δ should be understood as varying the cavity dimensions. In fact, B , ω_0 and P are the only parameters which can be externally controlled for a given dot-microcavity system.

Once we have precisely defined our equations, we may turn to the analysis of the simplest system, in which the dot may support only one pair.

A. A shallow dot with $N_{states} = 1$

This case was extensively studied in Ref. [2]. The authors obtain and solve the equations for the density matrix in a Fock basis composed by the electron-hole vacuum, $|G\rangle$, the exciton ground state, $|X\rangle$, and the n -photon states, $|n\rangle$. They write equations for the time evolution of the populations, $\rho_{Gn,Gn}$, $\rho_{Xn,Xn}$, and the coherences, $\rho_{Gn,Xn-1}$. To solve them, they should truncate the photon Hilbert space. For $n \leq 100$, for example, they have 300 equations. This is an exact treatment, in which the authors may compute correlation functions for the photon field, the spectrum of the emitted light, etc.

In our model, however, the $N_{states} = 1$ case is described by only three variables, ρ_1 , s , and the phase difference $\phi - \phi_1$. The photon field is assumed coherent. In spite of these simplifications, most of the results presented in paper [2] concerning the system dynamics are qualitatively and quantitatively reproduced by our equations. In the present section, we focus on new results, uncovered in paper [2].

The first feature we observe in our calculations is the presence of the three regimes, mentioned in [2], under

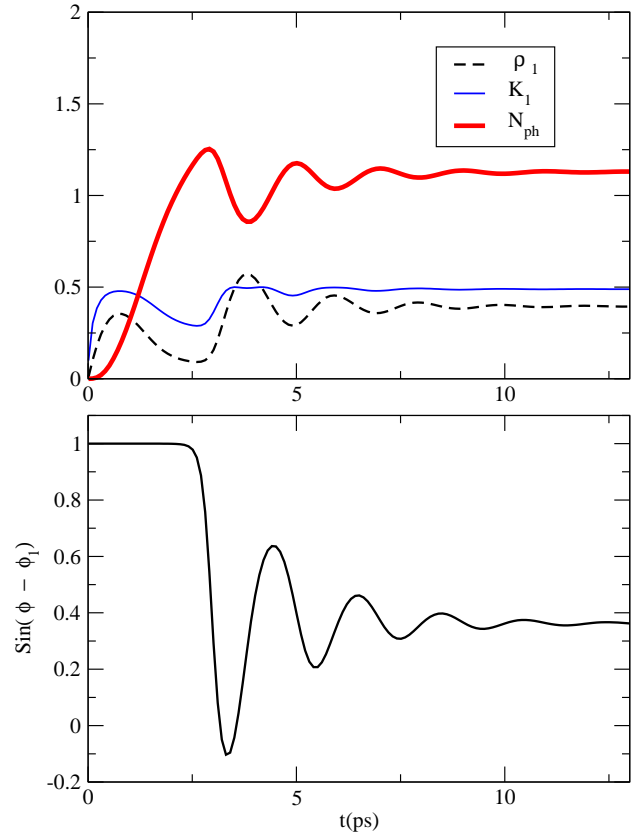


FIG. 1: (Color online) Number of photons, dot occupation and polarization in the one-pair dot for $P = 1 \text{ ps}^{-1}$, $\varkappa = 0.5 \text{ ps}^{-1}$. The photon energy is $\Delta = 4.5 \text{ ps}^{-1}$ (maximum resonance).

which the quantum dot - microcavity system may operate. They can be roughly classified according to the relation between pumping and losses: (i) $P \gg \varkappa$, (ii) $P \sim \varkappa$, and (iii) $\varkappa \gg P$.

We show in Fig. 1 an example of calculations corresponding to the intermediate regime (ii), in which $P = 1 \text{ ps}^{-1}$ and $\varkappa = 0.5 \text{ ps}^{-1}$. This example reveals oscillations in the transient interval until the asymptotic values are reached. The oscillations of the number of photons in the cavity are due to non compensation between the rates of creation of photons and losses, and even to photon absorption by the dot (when $\sin(\phi - \phi_1) < 0$).

The asymptotic number of photons, computed at $t_f = 100 \text{ ps}$ as a function of Δ for a high quality cavity ($\varkappa = 0.1$) is shown in Fig. 2. The pair frequency (pair energy divided by \hbar) in the present case is

$$\begin{aligned} \omega_{pair} &= \frac{1}{\hbar} \left(E_1^{(e)} + E_1^{(h)} + t_{11}^{(e)} + t_{11}^{(h)} \right) \\ &- \frac{\beta}{\hbar} \langle 1, 1 | r | 1, 1 \rangle = 4.5 \text{ ps}^{-1}. \end{aligned} \quad (27)$$

Extreme resonance corresponds to $\Delta = \omega_{pair}$. The dependence N_{ph} vs Δ in Fig. 2a ($P = 7 \text{ ps}^{-1}$) resembles

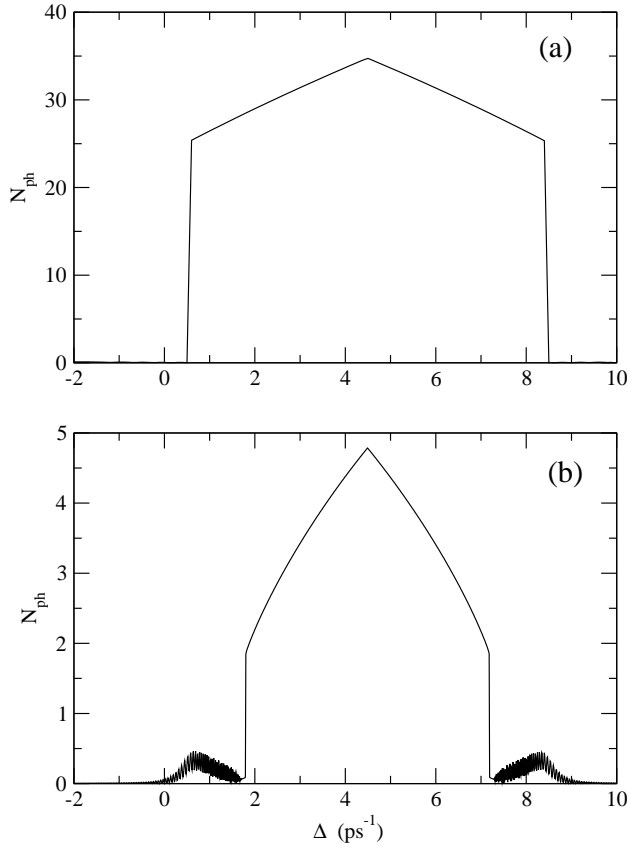


FIG. 2: The number of photons as a function of the photon energy for (a) $P = 7 \text{ ps}^{-1}$, $\varkappa = 0.1 \text{ ps}^{-1}$, and (b) $P = 1 \text{ ps}^{-1}$, $\varkappa = 0.1 \text{ ps}^{-1}$.

a step function with a mean value of 30 photons inside the resonance interval, and zero outside. If the cavity is such that the actual Δ lies in the abruptly varying region, small changes produced by variations in B or in ω_0 could switch between the two “states” of the cavity. Although the step-like variation could be an artifact of our simplified equations, an abrupt variation is expected.

Similar step-like variations are shown in Fig. 2b, which corresponds to $P = 1 \text{ ps}^{-1}$. In addition, outside the resonance interval there are asymptotic oscillating solutions, whose characteristic behavior is illustrated in Fig. 3 for $\Delta = 8 \text{ ps}^{-1}$. Notice that, in the oscillating solution, the quantum dot is periodically emitting ($\sin(\phi - \phi_1) > 0$) and absorbing ($\sin(\phi - \phi_1) < 0$) photons from the cavity with a period around 2.5 ps. The mean number of photons is only around 0.1, thus our coherent approximation could be very rough. Such periodic solutions are, however, very common in the larger systems with $N_{states} > 1$, as will be seen below.

From the point of view of the theory of nonlinear evolution differential equations¹³, in the resonance interval the solution of the system (14-17) is attracted by a stable critical point (an spiral), whereas the asymptotic periodic solution outside the resonance interval for Δ corresponds

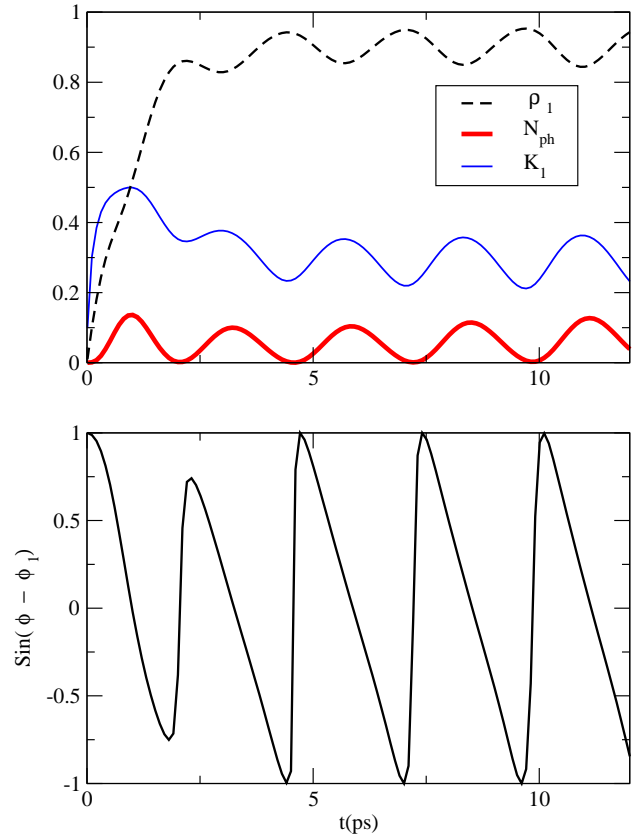


FIG. 3: (Color online) The same as in Fig. 1, but for $P = 1 \text{ ps}^{-1}$, $\varkappa = 0.1 \text{ ps}^{-1}$, and $\Delta = 8 \text{ ps}^{-1}$.

to a limit cycle. This view reveals the existence of a second stable attractor (also an spiral) in the resonance interval, which is not seen in calculations because the used initial conditions is not in its basin of attraction. As we move out of the resonance interval, one of the stable critical points disappears (a bifurcation) and the limit cycle emerges. In addition, at any value of Δ there is a third critical point of hyperbolic character (with one unstable states of the quantum dot-microcavity system, how to reach them, and even how to reach the hyperbolic point by using control of chaos¹³, the nature of the limit cycles, etc are very interesting questions which deserve further investigation. In the larger, $N_{states} > 1$, systems the dynamics is expected to be even more complex. In the present paper, we restrict the analysis to the situation with null initial conditions, described in Sec. II C, and leave the more general questions for a later work.

B. The $N_{states} = 2$ dot coupled to $\sigma_{(+)}$ light

In view of the fact that, in our equations, the $\sigma_{(+)}$ -polarized mode evolves independently of the $\sigma_{(-)}$ mode, the next nontrivial case corresponds to a dot which may

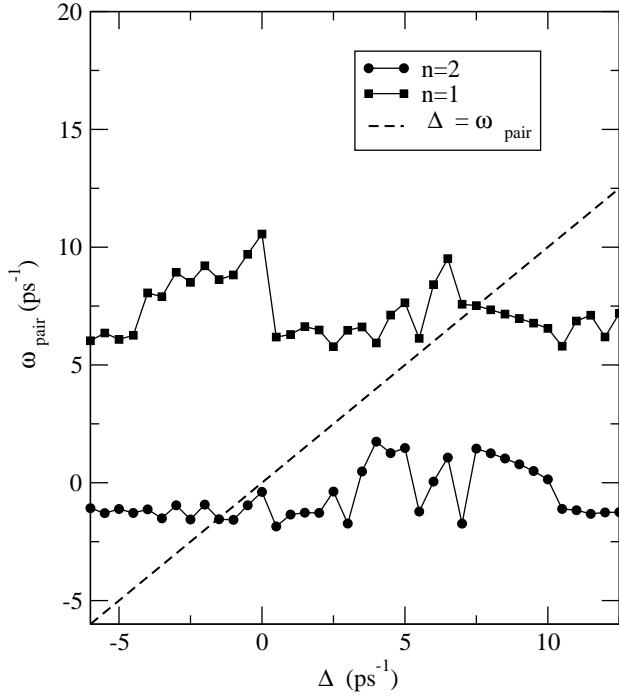


FIG. 4: The single-pair levels as a function of the photon energy for $P = 1 \text{ ps}^{-1}$, $\varkappa = 0.1 \text{ ps}^{-1}$.

support up to two pairs, $N_{states} = 2$, interacting with the same photon mode. To be specific, we will consider coupling to the $\sigma_{(+)}$ mode.

The dynamics, in many ways, has features very similar to those of the simpler one-pair system. In particular, the three operation regimes are observed. In addition, there are new characteristics, which are briefly outlined below.

The first new (expected) feature is the two-peak structure in the number of photons as a function of Δ as a result of individual resonances with the single-pair levels. Coulomb interactions are crucial in determining the position of these levels. Indeed, we have:

$$\begin{aligned} \omega_{pair}(n) = & \frac{1}{\hbar} \left(E_{gap} + E_n^{(e)} + E_{\bar{n}}^{(h)} + t_{n\bar{n}}^{(e)} + t_{\bar{n}n}^{(h)} \right) \\ & - \frac{\beta}{\hbar} \langle n, n | 1/r | n, n \rangle \\ & - \frac{2\beta}{\hbar} \sum_{j \neq n} \langle n, j | 1/r | j, n \rangle \rho_{j\downarrow}. \end{aligned} \quad (28)$$

In our model quantum dot, the pair frequencies at $\beta = 0$ are equal to 17.32 and 20.99 ps^{-1} . The account of Coulomb interactions move them to the interval from -2 to 10 ps^{-1} , as shown in Fig. 4, and make the single-pair levels dependent on the occupations ρ_n . But Coulomb interactions modify also the phases and occupations (see Eqs. (15) and (17)) causing strong changes in the stationary solutions. We illustrate in Fig. 5 these effects for the system with parameters $P = 1 \text{ ps}^{-1}$ and $\varkappa = 0.1$

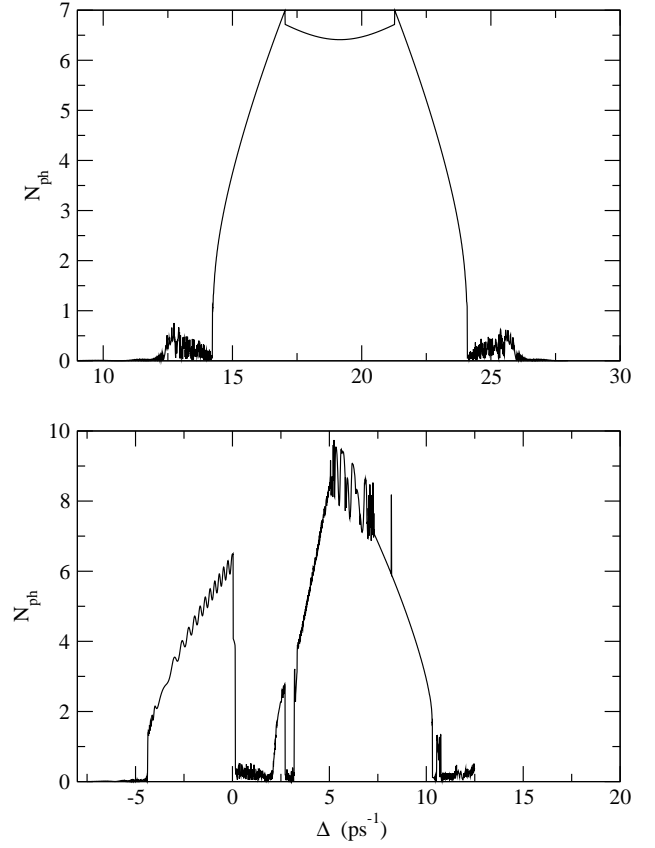


FIG. 5: The number of photons as a function of the photon energy for the $N_{states} = 2$ system with $P = 1 \text{ ps}^{-1}$, $\varkappa = 0.1 \text{ ps}^{-1}$. In the upper panel, Coulomb interactions are not included ($\beta = 0$).

ps^{-1} .

A second interesting characteristic is that asymptotic oscillatory solutions are very common, in particular inside the resonance intervals. It means that, as a rule, the number of photons and the occupations will vary periodically around a mean value. In our Fig. 5, where the number of photons is computed at fixed $t_f = 100 \text{ ps}$, oscillatory solutions are seen as apparently random behavior of N_{ph} .

It is interesting also to look at the relative phases, $\phi - \phi_i$ in each of the resonance intervals. Let us consider, for example, the system described in Fig. 5b. In the upper interval, $3 \lesssim \Delta \lesssim 10 \text{ ps}^{-1}$, the two single-pair levels emit or absorb almost in phase (see Fig. 6a). In the lowest interval, $-5 \lesssim \Delta \lesssim 0 \text{ ps}^{-1}$, one level is emitting, and the second one emits and absorb, but they do so “in phase”. That is, maximum emission occurs at the same time in both levels, and maximum absorption in one of them occurs at coincidence with minimum emission in the other. The situation is depicted in Fig. 6b. Finally, in the central peak around $\Delta \approx 2.5 \text{ ps}^{-1}$, which is the result of interference and disappears when parameters are changed, emission and absorption in the two levels are

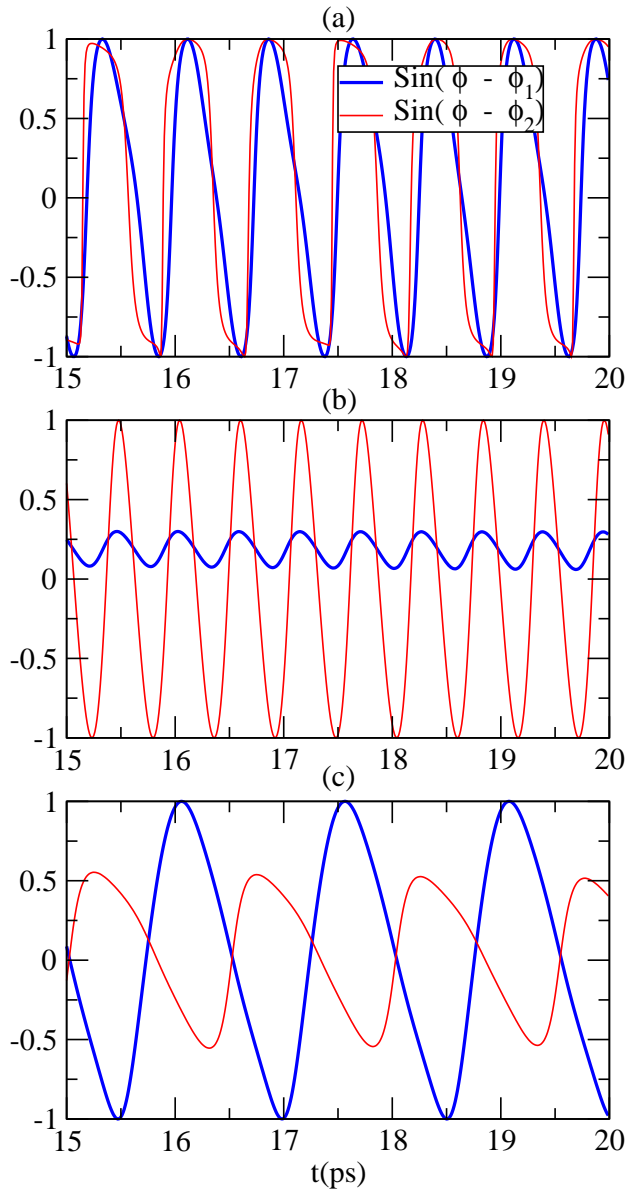


FIG. 6: (Color online) $\sin(\phi - \phi_i)$ in the $N_{states} = 2$ dot and cavity parameters $P = 1 \text{ ps}^{-1}$, $\varkappa = 0.1 \text{ ps}^{-1}$, and (a) $\Delta = 7 \text{ ps}^{-1}$, (b) $\Delta = -3 \text{ ps}^{-1}$, and (c) $\Delta = 2.5 \text{ ps}^{-1}$.

“in counterphase”, as can be seen in Fig. 6c. Notice that the periods of these oscillatory motions take values in the range between 0.5 and 1.5 ps. This means angular frequencies between 4 and 12 ps^{-1} . These numbers may be compared with the Rabi frequency, $g s/\hbar = 1.5 s \text{ ps}^{-1}$, which takes values around 2 - 4 ps^{-1} , and the characteristic frequency of Coulomb interactions, $\beta/\hbar \approx 10 \text{ ps}^{-1}$.

Let us stress that we are pumping both single-pair levels at the same rate, P . The qualitative features of the $N_{states} = 2$ problem, mentioned above, do not seem to rely on the specific pumping scheme used. The qualitative features do not change either when relaxation

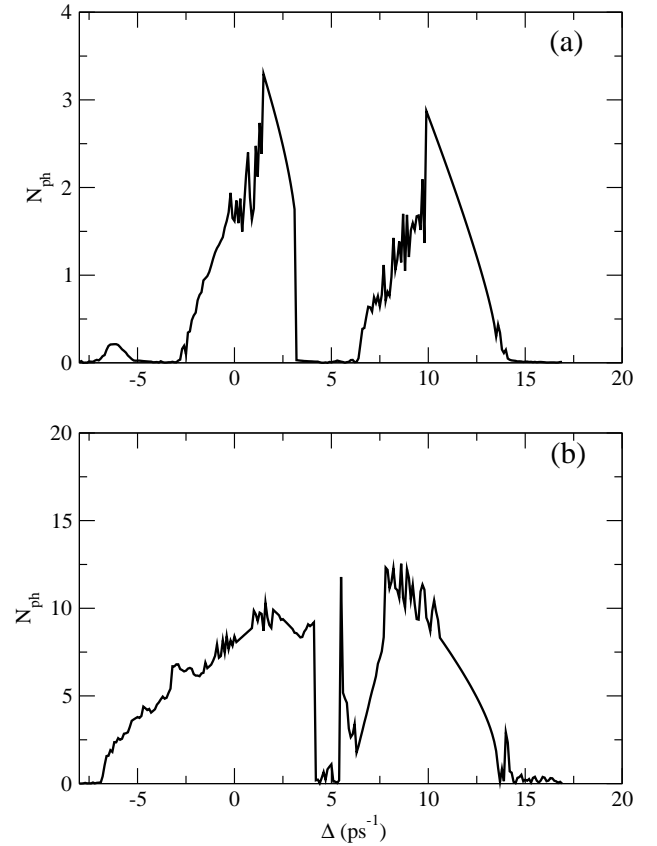


FIG. 7: Number of photons as a function of the photon energy for the $N_{states} = 3$ dot and cavity parameters (a) $P = 3 \text{ ps}^{-1}$, $\varkappa = 1 \text{ ps}^{-1}$, and (b) $P = 1 \text{ ps}^{-1}$, $\varkappa = 0.1 \text{ ps}^{-1}$.

from the higher-energy level to the lower-energy one is included.

C. The $N_{states} = 3$ dot coupled to $\sigma_{(+)}$ light

In general, the resonance curve, N_{ph} vs Δ , in the $N_{states} = 3$ system exhibits three peaks, as one can expect (Fig. 7a). For certain values of the system parameters, two or more peaks may overlap, or additional sharp peaks (the result of interference) may emerge (see, for example, Fig. 7b).

Concerning the relative phases between the polarization functions and the radiation field, $\phi - \phi_i$, one can roughly say the following. In the uppermost resonance interval, the three single-pair levels cooperate. This means that they are all emitting simultaneously, or periodically absorbing-emitting almost “in phase”. In the central interval, in general, there are two levels cooperating, and the third is not. For example, two of them are emitting, and the third is absorbing. Finally, in the lowest interval, when one of the levels is emitting, the second is absorbing, and the third alternates between the first two. Curves are qualitatively similar to the $N_{states} = 2$

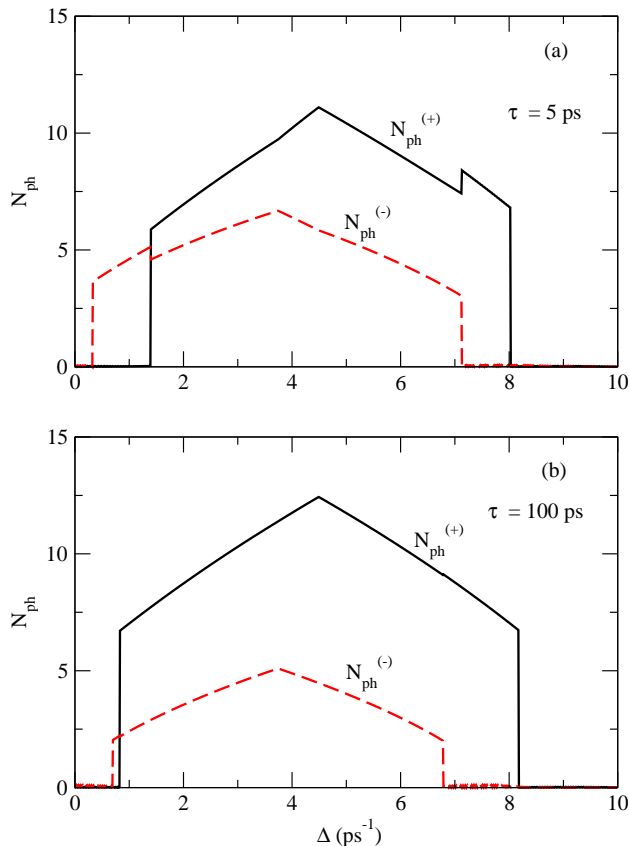


FIG. 8: (Color online) The $N_{states} = 2$ dot with spin-flip processes included: (a) $\tau_s = 5$ ps, (b) $\tau_s = 100$ ps. See explanation in the main text.

case, and will not be shown.

D. The $N_{states} = 2$ dot coupled to different photon modes

In this section, we consider the possibility of spin-flips between exciton states with a characteristic rate $2\pi/\tau_s$. Typical values of τ_s are around 5 ps or larger¹⁴. Then, there is a new nontrivial situation for the $N_{states} = 2$ dot, in which one electron-hole pair is coupled to the $\sigma_{(+)}$ photon mode, and the second one to the $\sigma_{(-)}$ mode.

The spin-flip term will be added to the equations for the occupations, Eq. (17). At $B = 7$ Teslas, the Zeeman splitting between exciton states is around 0.7 meV. The lowest exciton state is coupled to the $\sigma_{(-)}$ photon. Then, in the equation for $\rho_{1\downarrow}$ (the exciton coupled to the $\sigma_{(+)}$ photon), we add a term

$$-\frac{2\pi}{\tau_s}\rho_{1\downarrow}(1 - \rho_{1\uparrow}), \quad (29)$$

and for $\rho_{1\uparrow}$ a term

$$\frac{2\pi}{\tau_s}\rho_{1\downarrow}(1 - \rho_{1\uparrow}). \quad (30)$$

Notice the Pauli blocking factors in them. Spin-flip transitions from $\rho_{1\uparrow}$ to $\rho_{1\downarrow}$ would require an activation mechanism to overcome the energy barrier, and will not be included.

The results for the system with cavity parameters $\varkappa = 0.1$ ps⁻¹, $P_{(+)} = 5$ ps⁻¹, $P_{(-)} = 2$ ps⁻¹, are shown in Fig. 8. The lower figure corresponds to $\tau_s = 100$ ps, i.e., when the $\sigma_{(+)}$ and $\sigma_{(-)}$ dynamics are independent. The upper one, to $\tau_s = 5$ ps, that is, a rate $2\pi/\tau_s \approx 1.2$ ps⁻¹. Step-like variations in one of the photon populations are transmitted to the other photon number. Interesting enough is the region $0.4 < \Delta < 1.3$ ps⁻¹, where there are only $\sigma_{(-)}$ photons in spite of the fact that $P_{(+)} > P_{(-)}$.

IV. CONCLUDING REMARKS

We have explicitly written and numerically solved the evolution (Bloch-Lamb) equations describing the dynamics of a quantum dot-microcavity system. The main simplifications contained in our equations are the following: (a) they are mean field equations, i.e., do not contain particle-particle correlations, and (b) the photon field is coherent. Assumption (b) is closely related to (a). The reward from this simplified approach is that the system of equations is relatively small, allowing a qualitative analysis of its solutions and the extension to larger dots, which may support more than one electron-hole pair.

In the simplest system with $N_{states} = 1$, the qualitative analysis revealed the existence of resonance intervals for the parameters, where the coupling to the photon field of the cavity is optimal and the number of photons in the stationary state reaches a maximum. There is also a second stable stationary state, which is not reached because the used (null) initial conditions is not in its basin of attraction. The two stable solutions should be further analysed focusing on a possible optical bistability in this system¹⁵. Outside the resonance interval, one of the stable states disappears (suggesting a bifurcation) leading to the appearance of stable periodic orbits in which the physical magnitudes oscillate. In this oscillatory states, the quantum dot is periodically absorbing and emitting photons from and to the cavity. Under strong pumping, the transition resonance-out of resonance may be almost step-like, a fact which may also have interesting applications. We have left many questions unexplored such as, for example, the width of the resonance interval in Δ , or the transient time before the stationary state is reached, as functions of the system parameters.

Let us stress that the existence of two stable stationary solutions are intuitively related to the two possible couplings between an exciton and a photon (the two polariton branches in a quantum well under weak coupling, for example). However, we can not yet understand the

way they may arise from the system of linear equations of Ref. 2. We think that the truncation of the photon Fock space is responsible for this difference with our results.

Larger systems exhibit even more complex dynamics, which seems to strongly depend on the position of the single-pair levels. Most of the new features are already seen in the $N_{states} = 2$ dot, when both pair states are coupled to the same photon mode. We showed results for a dot in which the energy levels are 8 - 10 meV apart, in such a way that individual resonance intervals are resolved. Coulomb interactions are shown to have drastic effects, not only on the level positions, but also causing interferences and altering the very nature of the stationary states. Oscillatory states are reached almost for any values of the system parameters, even inside the resonance intervals. Cooperative or non cooperative behavior of the single-pair levels are obtained in different parameter regions. In the $N_{states} = 3$ system, these fea-

tures are reinforced.

The account of relaxation between electronic states or a change in the pumping scheme used to feed the dot are shown to have small impact on this qualitative and semi-quantitative picture. Other effects such as the coupling to the delocalized states of the wetting layer surrounding the self-assembled dot are to be considered. This coupling to the wetting layer is crucial in other contexts¹⁶.

Work along some of the abovementioned questions is currently in progress.

Acknowledgments

The authors acknowledge the Comitee for Research of the Universidad de Antioquia for support.

-
- ¹ D. Meschede, H. Walther, and G. Muller, Phys. Rev. Lett. **54**, 551 (1985).
- ² J.I. Perea, D. Porras, and C. Tejedor, <http://arxiv.org/cond-mat/0310570>.
- ³ J.M. Gerard, B. Sermage, B. Gayral, B. Legrand, E. Costard, and V. Thierry-Mieg, Phys. Rev. Lett. **81**, 1110 (1998).
- ⁴ G.S. Solomon, M. Pelton, and Y. Yamamoto, Phys. Rev. Lett. **86**, 3903 (2001).
- ⁵ M. Pelton, C. Santori, J. Vuckovic, B. Zhang, G.S. Solomon, J. Plant, and Y. Yamamoto, Phys. Rev. Lett. **89**, 233602 (2002).
- ⁶ O. Benson, C. Santori, M. Pelton, and Y. Yamamoto, Phys. Rev. Lett. **84**, 2513 (2000).
- ⁷ T.M. Stace, G.J. Milburn, and C.H.W. Barnes, Phys. Rev. **B 67**, 085317 (2003).
- ⁸ J.M. Gerard, D. Barrier, J.Y. Marzin, R. Kuszelewicz, L. Manin, E. Costard, V. Thierry-Mieg, and T. Rivera, Appl. Phys. Lett. **69**, 449 (1996).
- ⁹ A. Yariv, Optical Electronics (Saunders College, San Francisco, 1991).
- ¹⁰ G. Bastard, *Wave mechanics applied to semiconductor heterostructures* (Les editions de physique, Les Ulis Cedex, 1998).
- ¹¹ H. Haug and S.W. Koch, *Quantum Theory of the Optical and Electronic Properties of Semiconductors* (World Scientific, Singapore, 1994).
- ¹² M.O. Scully and S. Zubairy, *Quantum Optics* (Cambridge Univ. Press, Cambridge, 2001).
- ¹³ E. Ott, *Chaos in Dynamical Systems* (Cambridge Univ. Press, Cambridge, 2002).
- ¹⁴ J.M. Kikkawa and D.D. Awschalom, Phys. Rev. Lett. **80**, 4313 (1998).
- ¹⁵ M. Gurioli, L. Cavigli, G. Khitrova, and H. Gibbs, Phys. Stat. Sol. (a) **201**, 661 (2004).
- ¹⁶ Q.Q. Wang, A. Muller, P. Bianucci, E. Rossi, Q.K. Xue, T. Takagahara, C. Piermarocchi, A. H. MacDonald, and C.K. Shih, <http://arxiv.org/cond-mat/0404465>.